XIV International Conference on Computational Plasticity. Fundamentals and Applications
COMPLAS XIV
E. Oñate, D.R.J. Owen, D. Peric & M. Chiumenti (Eds)

COUPLED H-M FRACTURE INTERACTION USING FEM WITH ZERO-THICKNESS INTERFACE ELEMENTS

D. GAROLERA*, J.M. SEGURA†, I. CAROL*, M.R. LAKSHMIKANTHA† AND J. ALVARELLOS†

* Dept. of Civil and Environmental Eng., Div. of Geotechnical Eng.
BarcelonaTech (UPC), Campus Nord UPC, 08034 Barcelona, Spain
e-mail: daniel.garolera(a).upc.edu and ignacio.carol(a)upc.edu

†Repsol Technology Centre
28935 Móstoles (Madrid), Spain

Key words: zero-thickness interface, hydraulic fracture interaction, hydro-mechanic coupling

Abstract. Intensive hydraulic fracturing is a procedure employed for low permeability reservoir stimulation. This technique consists of generating a sequence of regularly spaced parallel fractures (multi-stage fracturing). The generation of a fracture involves the modification of the local stress state, and therefore, in the case of multi-stage fracturing, the propagation of a certain fracture can be affected by the injection sequence, as it has been observed with microseismicity monitoring [1]. This paper describes a study of this technique by means of the Finite Element Method with zero-thickness interface elements for the geo-mechanical modelling of discontinuities [2]. The technique consists in inserting interface elements in between standard elements to allow jumps in the displacement solution fields. For the mechanical problem, their kinematic constitutive variables are relative displacements, and the corresponding static variables are stress tractions. The relationship between variables is controlled via a fracture-based constitutive law with elasto-plastic structure [3]. Concerning the hydraulic problem, the interface formulation includes both the longitudinal flow (with a longitudinal conductivity parameter strongly dependent on the fracture aperture), as well as and the transversal flow across the element [4]. Previous work by the authors focused on the validation of the method, the analysis a single fracture plane problem [5, 6]. In this case the method is extended to allow free propagation of fractures in any direction, by means of inserting interface elements between all continuum elements. The results presented in this paper analyse the effect of material properties, in particular fracture characterization, in the propagation and the effect of different major to minor principal horizontal stress ratio, on the trajectory and interaction of the fractures.

1 INTRODUCTION

Advanced modelling of reservoir geo-mechanics involves the numerical representation of geological discontinuities. In the approach described in this paper, zero-thickness interface elements of the Goodman type [2] are considered for this purpose. Those elements can also be used for representing the fluid flow and the coupled hydro-mechanical problem [7]. The technique consists in inserting interface elements in between standard elements to allow jumps in the solution fields. For the mechanical problem, their kinematic constitutive (strain-type) variables are relative displacements, and the corresponding static (stress-type) variables are stress tractions. The relationship between variables is controlled via a fracture-based constitutive law with elasto-plastic structure [3]. Concerning the hydraulic problem, the interface formulation includes both the longitudinal flow (with a longitudinal conductivity parameter strongly dependent on the fracture aperture, cubic law), as well as and the transversal flow across the element (and an associated localized pressure drop, with the corresponding transversal conductivity parameter).

The study presented in this paper is an extension of recent work presented by the authors [4, 5, 6] which was verified first by comparison to existing analytical and numerical solutions for the propagation of a single hydraulic fracture [8].

2 HYDROMECHANICAL FORMULATION FOR ZERO-THICKNESS INTERFACE ELEMENTS

Present work follows the definition of zero-thickness interface element originally proposed in [9]. The main characteristic of this type of element is that one of its dimensions has collapsed. Therefore the integration is reduced in one order, line integration for 2D and surface integration for 3D. The mid-plane surface is defined via isoparametric interpolation on the basis of the coordinates of the mid-points, or points at mid-distance between each pair of nodes. This interpolation is based on a set of local coordinates ξ, η for the mid-plane surface in 3D, or ξ for the mid-plane line in 2D.

Nodal unknowns are transformed into mid-plane variables which represent variations (jumps or drops) of field variables. Mid-plane variables are expressed in terms of the local orthogonal coordinates system, presented in section 2.1. Then, the HM formulation is shown in section 2.2.

2.1 Zero-thickness variables

The nodal variables in a hydro-mechanical problem include the nodal displacements ($\mathbf{u}_e$) and the nodal fluid pressures ($\mathbf{p}^f{}_e$). The nodal (absolute) displacements are transformed into normal (r_n) and shear (r_{l_1}, r_{l_2}) relative displacements, which have the meaning of displacements jumps across the discontinuity. The other variable, fluid pressure, is transformed into two components, the average pressure ($\bar{p}^f_J$) and the pressure drop ($\check{p}^f_J$), across the discontinuity. A description of these variables and their conjugates is provided in the following paragraphs.

The relative displacement at a mid-plane point (ξ, η) of the discontinuity is denoted

as:

$$\mathbf{r} = \begin{pmatrix} r_n & r_{l_1} & r_{l_2} \end{pmatrix}^{\mathsf{T}} \tag{1}$$

where r_n is the normal component and the $r_{l_{(*)}}$ are the tangential components. These relative displacements and the corresponding stress variables are depicted in Fig. 1.

The relation between relative displacements and nodal displacements is given by the the following expressions:

$$\mathbf{r} = \mathbf{R}\, \mathbf{N}_{\text{J}}^{u}\, \mathbb{T}^{u}\, \mathbf{u}_e = \mathbf{B}_{\text{J}}\, \mathbf{u}_e \tag{2}$$

where $\mathbf{R}$ is the rotation matrix that transforms vector components into local orthogonal axes, $\mathbf{N}_{\text{J}}^{u}$ is matrix of nodal shape functions evaluated at integration position (ξ, η), and $\mathbb{T}^{u}$ is the "transformation" matrix, which generates the difference between bottom and top face of interface element.

Then, the $\mathbf{B}_{\text{J}}$ matrix is defined in analogy to the classical FEM continuum elements.

$$\mathbf{B}_{\text{J}} = \mathbf{R}\, \mathbf{N}_{\text{J}}^{u}\, \mathbb{T}^{u} \tag{3}$$

The matrix of nodal shape functions is defined in Eq. (4), where m is the number of nodes at midplane (which is half of the number of nodes of the interface element n) and d represents the number of mechanical degrees of freedom per node. The operator "$\otimes$" indicates the Kronecker product.

$$\mathbf{N}_{\text{J}}^{u} = \begin{pmatrix} N_1 & N_2 & \cdots & N_m \end{pmatrix} \otimes \mathbf{I}_d \tag{4}$$

The mechanical transformation matrix for the mechanical problem is defined as:

$$\mathbb{T}^{u} = \begin{pmatrix} -\mathbf{I}_m & \mathbf{I}_m \end{pmatrix} \otimes \mathbf{I}_d \tag{5}$$

The conjugate variables to the relative displacements are the stress tractions at the discontinuity mid-plane ($\boldsymbol{\sigma}_{\text{J}}$), which, for a specific point (ξ, η) of that surface, may be expressed as:

$$\boldsymbol{\sigma}_{\text{J}} = \begin{pmatrix} \sigma_n & \tau_{l_1} & \tau_{l_2} \end{pmatrix}^{\mathsf{T}} \tag{6}$$

where σ_n is the normal stress and τ_{l_1} and τ_{l_2} are the tangential components.

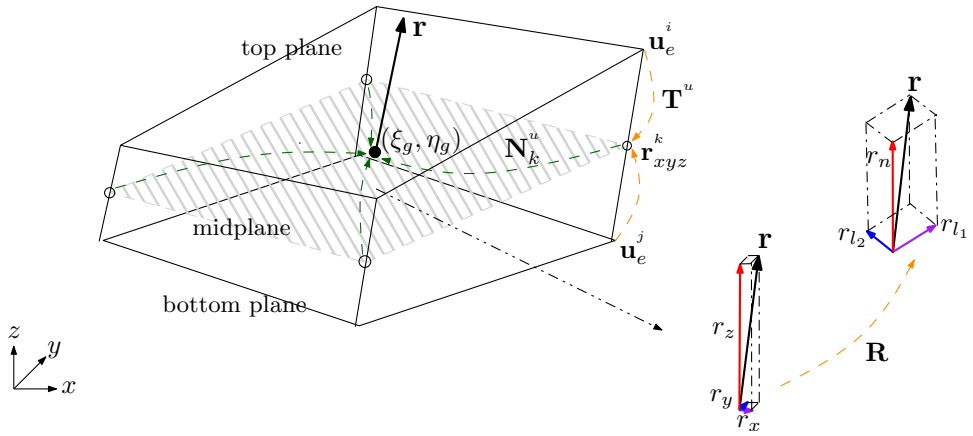

Figure 1: Relative displacements of zero-thickness interface element.

The average fluid pressure ($\bar{p}^f_{\text{J}}$) at a given point (ξ, η) of the discontinuity is obtained as the average between bottom and top fluid pressures and it can be expressed as:

$$\bar{p}^f_{\text{J}} = \mathbf{N}^{p\mathsf{T}}_{\text{J}}\ \mathbb{T}^p_L\ \mathbf{p}^f{}_e \tag{7}$$

$$\mathbf{N}^p_{\text{J}} = \begin{pmatrix} N_1 & N_2 & \cdots & N_m \end{pmatrix} \tag{8}$$

$$\mathbb{T}^p_L = \frac{1}{2}\begin{pmatrix} \mathbf{I}_m & \mathbf{I}_m \end{pmatrix} \tag{9}$$

The fluid pressure drop at the same point is given by the difference between top and bottom fluid pressures at element nodes:

$$\check{p}^f_{\text{J}}\big|_\xi = \mathbf{N}^{p\mathsf{T}}_{\text{J}}\ \mathbb{T}^p_T\ \mathbf{p}^f{}_e \tag{10}$$

$$\mathbb{T}^p_T = \begin{pmatrix} -\mathbf{I}_m & \mathbf{I}_m \end{pmatrix} \tag{11}$$

2.2 Finite element method formulation

This section describes the weak form of the equilibrium/continuity used for the implementation of zero-thickness interface elements. This equations are obtained from the application of Virtual work Principle. and the details can be found in [7]. The notation follows the terminology used in [10]:

$$\int_{\Omega_j} \mathbf{B}_{\text{J}}{}^{\mathsf{T}}\ \boldsymbol{\sigma}'_{\text{J}}\, d\Omega_j + \mathbf{Q}_{\text{J}}\ \mathbf{p}^f{}_e = \mathbf{f}^u_{\text{J}} \tag{12}$$

$$\mathbf{H}_{\text{J}}\ \mathbf{p}^f{}_e + \mathbf{S}_{\text{J}}\frac{\partial\, \mathbf{p}^f{}_e}{\partial t} + \mathbf{Q}_{\text{J}}{}^{\mathsf{T}}\frac{\partial\, \mathbf{u}_e}{\partial t} = \mathbf{f}^p_{\text{J}} \tag{13}$$

in which $\mathbf{Q}_{\text{J}}$ is the coupling matrix, $\mathbf{H}_{\text{J}}$ the diffusion matrix, $\mathbf{S}_{\text{J}}$ the storage matrix, and $\mathbf{f}^u_{\text{J}}$, $\mathbf{f}^p_{\text{J}}$ are the initial force and flow vector, with expressions:

$$\mathbf{Q}_{\text{J}} = \mathbb{T}^{u\mathsf{T}} \left(\int_{\Omega_{\text{J}}} \mathbf{N}^{u\mathsf{T}}_{\text{J}} \, \mathbf{R}^{\mathsf{T}} \, \alpha_{\text{J}} \, \mathbf{m}_{\text{J}} \, \mathbf{N}^p_{\text{J}} \, d\Omega_{\text{J}} \right) \mathbb{T}^p_L \tag{14}$$

$$\mathbf{H}_{\text{J}} = \mathbf{H}^p_{\text{J}_T} + \mathbf{H}^p_{\text{J}_L} = \tag{15}$$

$$= \mathbb{T}^{p\mathsf{T}}_T \left(\int_{\Omega_{\text{J}}} \mathbf{N}^{p\mathsf{T}}_{\text{J}} \, \check{K}_t \, \mathbf{N}^p_{\text{J}} \, d\Omega_{\text{J}} \right) \mathbb{T}^p_T + \mathbb{T}^{p\mathsf{T}}_L \left(\int_{\Omega_{\text{J}}} \left(\frac{\partial \, \mathbf{N}^p_{\text{J}}}{\partial \boldsymbol{x}_{\text{J}}} \right)^{\mathsf{T}} \frac{(-T^f_l)}{\gamma_f} \frac{\partial \, \mathbf{N}^p_{\text{J}}}{\partial \boldsymbol{x}_{\text{J}}} \, d\Omega_{\text{J}} \right) \mathbb{T}^p_L$$

$$\mathbf{S}_{\text{J}} = \mathbb{T}^{p\mathsf{T}}_L \left(\int_{\Omega_{\text{J}}} \mathbf{N}^{p\mathsf{T}}_{\text{J}} \, \frac{1}{M_{\text{J}}} \, \mathbf{N}^p_{\text{J}} \, d\Omega_{\text{J}} \right) \mathbb{T}^p_L \tag{16}$$

$$\mathbf{f}^u_{\text{J}} = \mathbb{T}^{u\mathsf{T}} \int_{\Gamma} \mathbf{N}^{u\mathsf{T}}_{\text{J}} \, \boldsymbol{\sigma}^{'}_0 \, d\Gamma \tag{17}$$

$$\mathbf{f}^p_{\text{J}} = \mathbb{T}^{p\mathsf{T}}_L \int_{\Omega_j} \left(\frac{\partial \, \mathbf{N}^p_{\text{J}}}{\partial \boldsymbol{x}_{\text{J}}} \right)^{\mathsf{T}} \frac{(-T^f_l)}{\gamma_f} \frac{\partial z}{\partial \boldsymbol{x}_{\text{J}}} \, d\Omega_j + \mathbb{T}^{p\mathsf{T}}_L \int_{\Gamma^f_q} \mathbf{N}^{p\mathsf{T}}_{\text{J}} \, \tilde{Q}^{\prime f} \, d\Gamma \tag{18}$$

where α_{J} is the Biot's coefficient, $\mathbf{m}_{\text{J}} = (1 \; 0 \; 0)^{\mathsf{T}}$, $\check{K}_t$ the transversal conductivity, T^f_l the longitudinal transmissivity, γ_f the specific fluid weight, M_{J} the Biot's modulus and $\tilde{Q}^{\prime f}$ the discharge per unit width.

3 STUDY OF FIVE-STAGE HF IN 2D

The study presented in this section is the analysis of multiple interacting hydraulic fractures using an academic example of 5 fracture jobs. The purpose of this study is to show the influence of previous hydraulic fractures on a subsequent fracture.

As said before, the interaction between different fracture jobs is due to the modification of local effective stress field. This variation is caused by the redistribution of stresses due to the fracture propagation and to the variation of fluid pressure after pumping.

The principal factors involved in this modelling are:

- The material properties of the rock (mechanical and fluid properties)
- The production design (spacing between jobs, volume of fluid injected, rate of injection, sequence of jobs, etc.).
- The initial stress state (vertical, horizontal maximum and minimum.)

Table 1: Material properties of continuum.

Parameter		*Value*	*Units*
E	Young's modulus	14400	MPa
ν	Poisson's ratio	0.2	-
K	Hydraulic conductivity	1×10^{-15}	$\mathrm{m\,s^{-1}}$
Ks	Solid compressibility	36000	MPa
α	Biot coef.	1.0	-

3.1 Model description

3.1.1 Geometry

A simplified configuration of five fracture jobs in a horizontal perforation is considered (see Fig. 2). In the current model the domain considered for the numerical analysis is composed of two subdomains (see Fig. 3):

- A *fractured subdomain*, which includes the zone in which the fractures can propagate (Fig. 3b), is discretized with a relatively dense FE mesh in which a network of interfaces is pre-inserted in between most continuum elements (Fig. 3c), with the purpose of allowing for sufficient freedom in the propagation of the fractures without predefined initial directions.

- A *continuum subdomain*, which corresponds to the surrounding domain farer from the fractures themselves, and consists of a layer or continuum elements without interfaces (Fig. 3a). This second subdomain is included in order to ensure the correct application of the boundary conditions (*in situ* stress and initial fluid pressure).

In this model the injection points are distributed along the x-axis (horizontal well) with fixed spacing of 5 m. Finally, as a first (2D) approach, the analysis is performed assuming plane strain conditions. Note that in order to avoid perturbations due to boundary conditions, the external boundary is placed around 200 m away from the interest area. In the fractured subdomain (Fig. 3b) zero-thickness interface elements are introduced between each pair of continuum elements. To ensure compatibility between the two subdomains, elastic interface elements are introduced all along the perimeter between the (outer) continuous and the (inner) fracture subdomains.

3.1.2 Material properties

The material properties used in the simulations are given below. For the continuum elements, an elastic isotropic material is assumed. Regarding the hydraulic behaviour, a practically impervious material is selected. All parameters are displayed in Table 1.

For the mechanical behaviour of the interface elements, normal and shear stiffness are assigned high values. These parameters may be understood as penalty coefficients with high values in order to avoid excessive unrealistic elastic deformations at the interfaces.

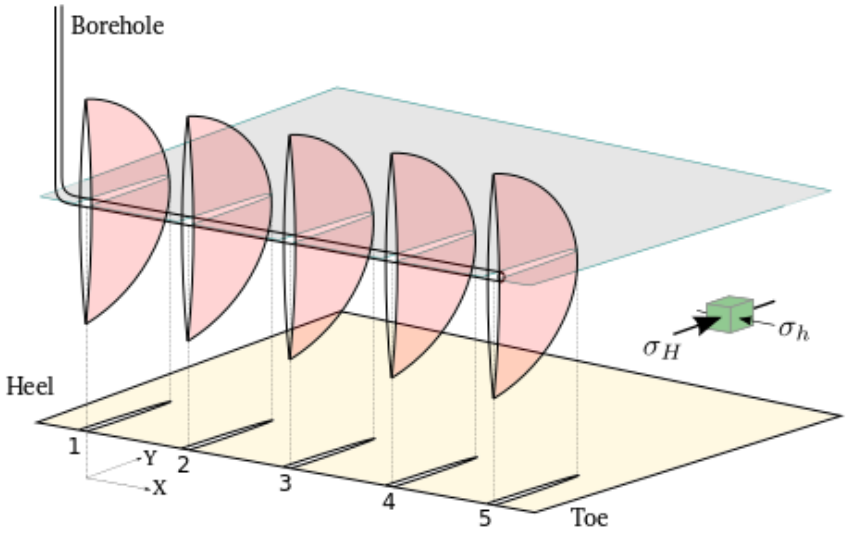

Figure 2: Scheme of 5 fracture job test.

Therefore, in practice the resulting deformation of the fractures can be assumed to represent almost exclusively the inelastic behaviour, that is, crack opening and shear slip.

The constitutive model used for the fractures is the elastoplastic constitutive formulation with fracture energy-based evolution laws described in detail in [3]. Low values of strength (tensile strength and cohesion) are selected in order to simulate existing fractures with very low or practically null cohesion [8]. The hydraulic behaviour of the interface is controlled by the so-called cubic law. The summary of interface parameters is shown in Table 2.

3.1.3 Boundary conditions

The boundary conditions are applied in a sequence of six steps (see Fig. 4):

Step 1: Stress initialization. In this step, a distributed load is applied over the external boundary: 1.0 MPa is imposed in the y-direction (σ_H). For the x-axis three cases are considered: 0.5 MPa, 0.7 MPa and 0.9 MPa (values of σ_h). The difference of principal stresses ensures that the preferential fracture direction is the y-direction (see Fig. 4, first row).

Steps 2-6: Single fracture jobs. A flow rate of $Q = 0.001\,\mathrm{m}^3/\mathrm{s}$ is injected at the injection point during 25 s. This step is repeated starting from job 1 and finishing at job 5 (see Fig. 4, second row)

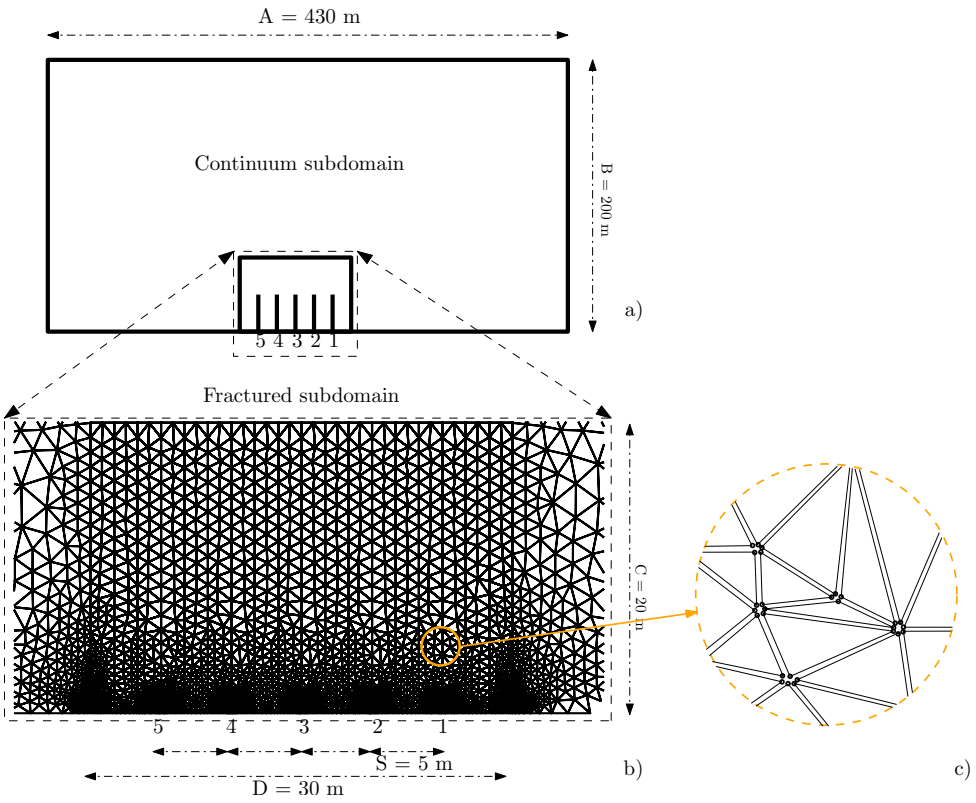

Figure 3: Model geometry for 5 fracture job test; a) full domain; b) fractured subdomain with detail of injection points position; and c) detail of network of interface elements inserted between continuum element. All dimensions are in meters.

3.2 Numerical Results and discussion

As already said, the objective of this study case was to learn about the interaction between subsequent fracturing jobs. The interaction is caused by the modification of the effective stress field during fracture propagation. For this purpose, several computations were performed focusing the interest on the effect of the *in situ* stress anisotropy. In particular, three cases with different ratio between maximum (σ_H) and minimum (σ_h) horizontal stress were run. All calculations assume the same maximum compression applied along the y-axis (on top and bottom limits of the domain), and different levels of minimum compression applied over the x-axis: a high anisotropic case $0.5\sigma_H$, a medium anisotropy case $0.7\sigma_H$ and a low anisotropy case $0.9\sigma_H$.

Figure 5 shows the evolution of fluid pressure at the injection points (crack mouths) along the entire simulation for the low anisotropy case. It is observed that the peak pressure for each injection is higher than the previous one, due to the increment of stress confinement after the previous fracture job. Therefore, the pressure necessary for opening the fracture increases due to the interaction of jobs, that is, the sequential scheme of injections causes a slow but gradual increase of the subsequent injection pressures.

Figure 6 shows the fluid pressure distribution at the end of fith fracture job, for the

Table 2: Material properties of interfaces.

Parameter		*Value*	*Units*
K_n	Normal stiffness	1×10^{-6}	$\mathrm{MPa\,m^{-1}}$
K_{t_1} and K_{t_2}	Tangentials stiffness	1×10^{-6}	$\mathrm{MPa\,m^{-1}}$
χ_0	Tensile strength	0.05	MPa
$\tan(\phi)$	Friction angle	0.2 (11.3°)	
c_0	Cohesion	0.5	MPa
G_f^I	Energy mode I	0.001	MPa m
G_f^{IIa}	Energy mode IIa	0.01	MPa m
T_{l_0}	Ini. Long. transmi.	0.0	$\mathrm{m^2/s}$
K_t^p	Trans. conduc.	1.0	$\mathrm{s^{-1}}$

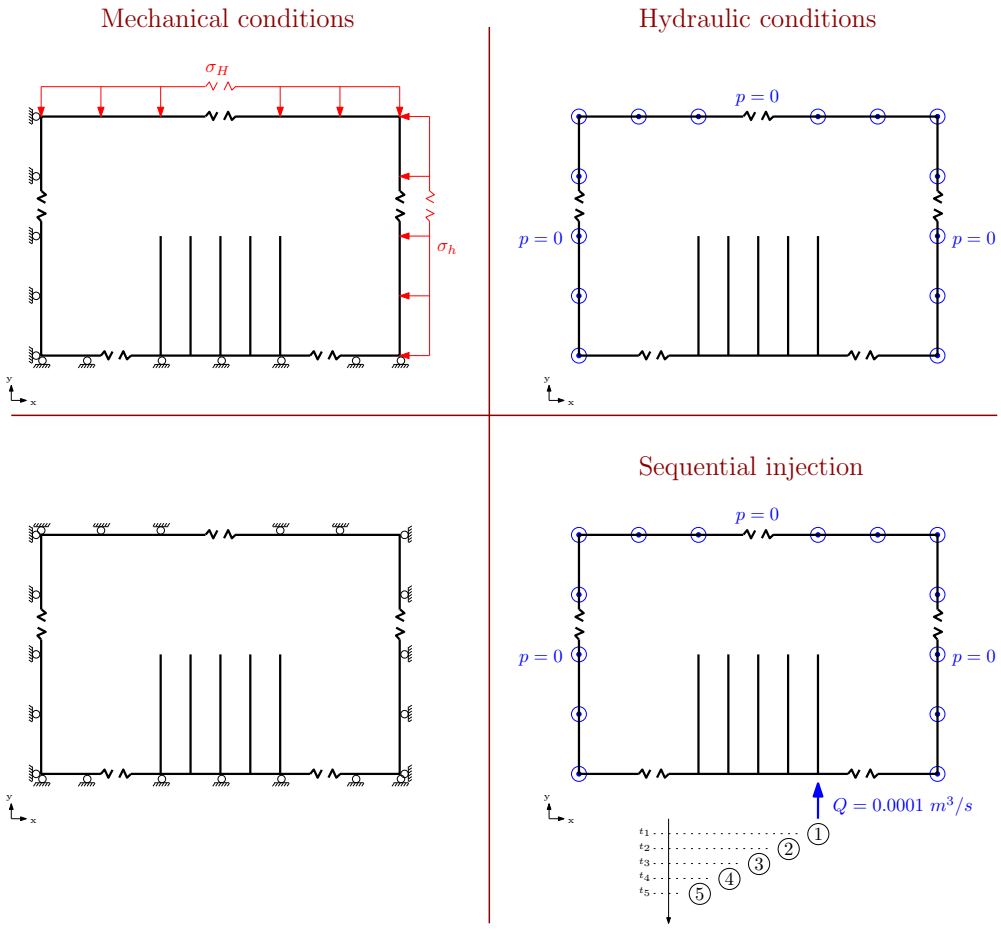

Figure 4: Boundary conditions for mechanical (left column) and flow (right column), for each of all the steps of the analysis (rows) in the two injection sequences considered.

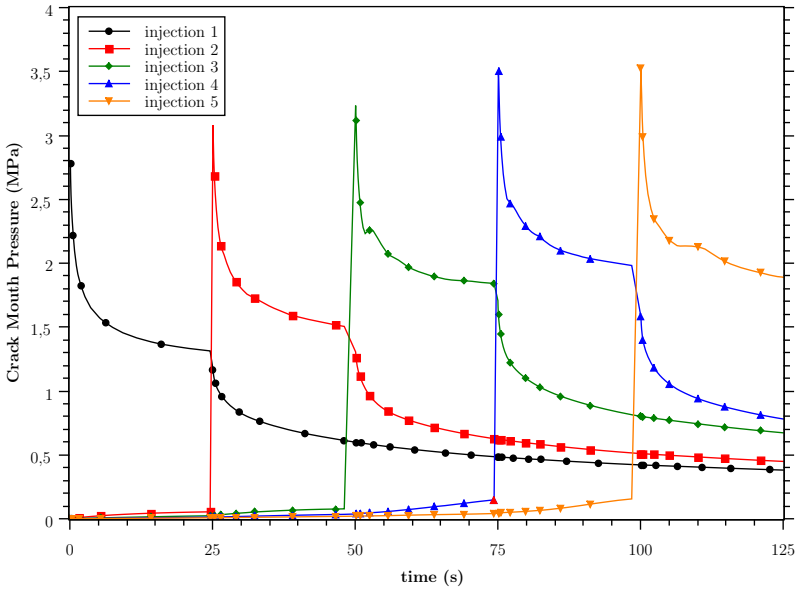

Figure 5: Crack Mouth Pressure evolution after 5 fracture jobs. Case $\sigma_h/\sigma_H = 0.9$

various σ_h/σ_H ratios scenarios. For a given *in situ* stress ratio, a slight interaction between fractures may seem to start appearing already from the second injection, although a clear interaction is not observed until the fifth injection for the high anisotropy case and until the third injection for the low anisotropy case, when the fracture clearly deviates from the initial vertical trajectory.

It is possible that these results may be slightly affected by the mesh layout, although after various tentative calculations these effects seem not to be very significant.

The results demonstrate that fracture interaction is clearly more pronounced as the difference between principal stresses is lower. For instance, the third injection in the case with ratio 0.9 shows a deviation of the last fractures which is not detected for ratios 0.7 and 0.5 until the fifth job and with much lower intensity.

4 CONCLUDING REMARKS

A methodology for 2D analysis of multi-stage hydraulic fracture is presented through the use of zero-thickness interface elements with full HM coupling. In this study an academic example of five fracture jobs in 2D is analysed in order to investigate the interaction between diffents jobs as observed in the field. Among all the variables involved in the interaction between fracture jobs, this paper has focused on the effect of different *in situ* stress states in terms of maximum-to-minimum horizontal stress ratio. The results presented in this paper show a clear interaction between different jobs, with more pronounced effects when the two horizontal stresses tend to be similar.

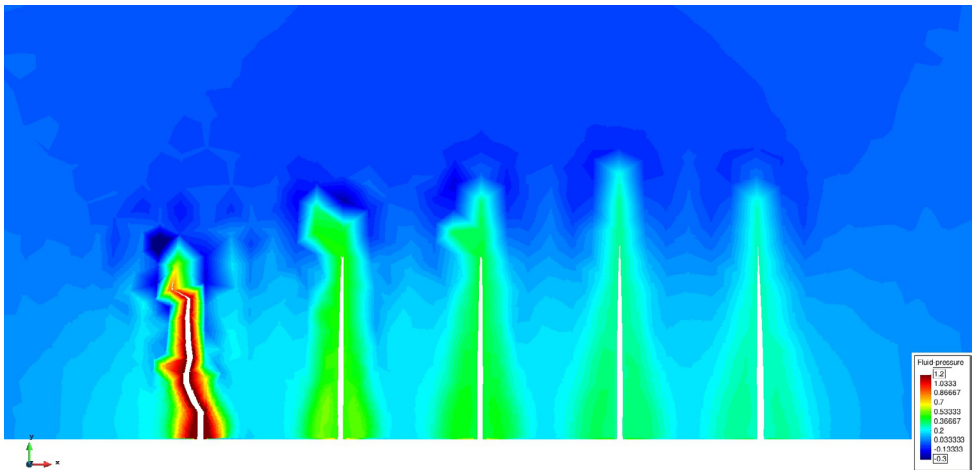

(a) $\sigma_h/\sigma_H = 0.5$

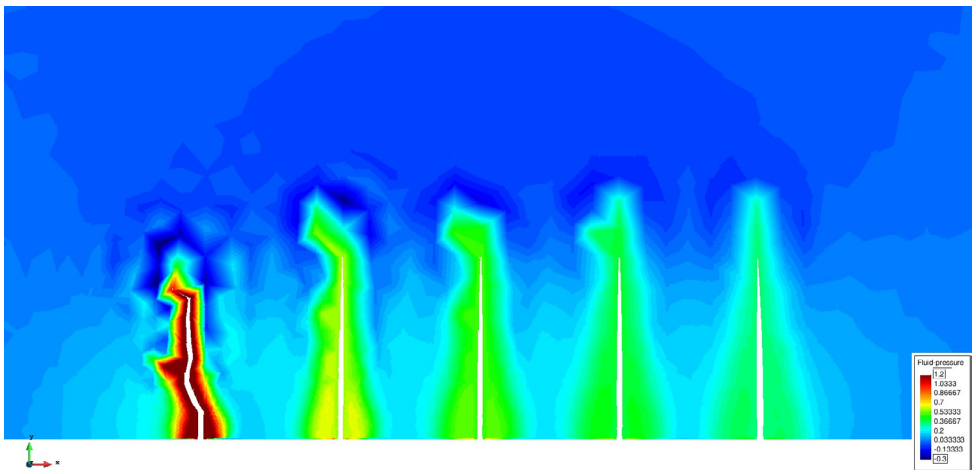

(b) $\sigma_h/\sigma_H = 0.7$

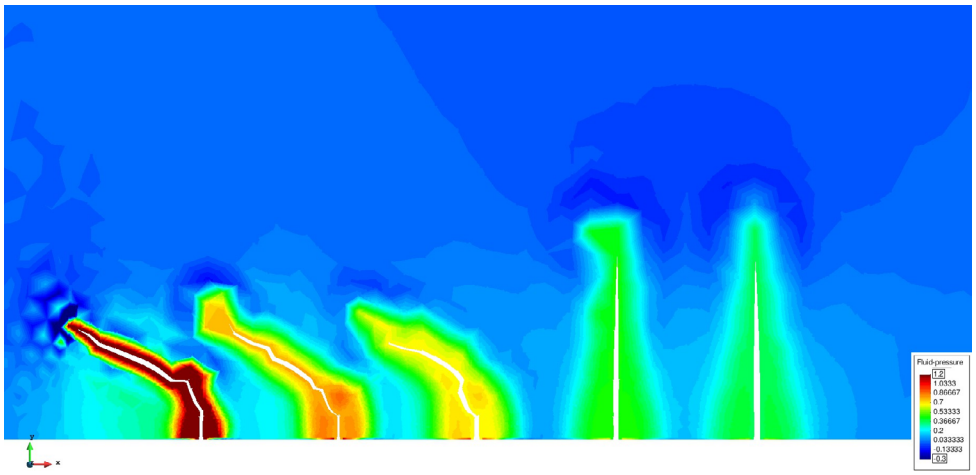

(c) $\sigma_h/\sigma_H = 0.9$

Figure 6: Effect of stress anisotropy on fracture interaction for different stress ratios: a) $\sigma_h/\sigma_H = 0.5$, b) $\sigma_h/\sigma_H = 0.7$ and c) $\sigma_h/\sigma_H = 0.9$. Fluid pressure distribution at time 125s.

5 ACKNOWLEDGEMENTS

The work was partially supported by research grants BIA2016-76543-R from MEC (Madrid), which includes FEDER funds, and 2014SGR-1523 from Generalitat de Catalunya (Barcelona). The support from REPSOL for this research is also greatfully acknowledged.

REFERENCES

[1] J. Daniels, G. Waters, J. Le Calvez, D. Bentley, and J. Lassek. Contacting more of the barnett shale through an integration of real-time microseismic monitoring, petrophysics, and hydraulic fracture design. *SPE-110562-MS*, 2007.

[2] A. Gens, I. Carol, and E. Alonso. A constitutive model for rock joints formulation and numerical implementation. *Computers and Geotechnics*, 9:3–20, 1990.

[3] I. Carol, P. Prat, and C. López. A normal/shear cracking model. application to discrete crack analysis. *ASCE J. Engrg. Mech.*, 123(8):765–773, 1997.

[4] J. M. Segura and I. Carol. Coupled hm analysis using zero-thickness interface elements with double nodes. Part II: Verification and application. *International Journal for Numerical and Analytical Methods in Geomechanics*, 32(18):2103–2123, 2008.

[5] D. Garolera, I. Aliguer, J. Segura, I. Carol, M. Lakshmikantha, and J. Alvarellos. Hydro-mechanical coupling in zero-thickness interface elements, formulation and applications in geomechanics. In *Proceedings of EUROCK 2014*, pages 1379–1384. CRC Press, 2014.

[6] D. Garolera, J. Segura, I. Carol, M. Lakshmikantha, and J. Alvarellos. Hydro-mechanical coupling in zero-thickness interface elements, formulation and applications in geomechanics. In *Proceedings of COMPLAS 2015*, pages 1379–1384. CIMNE, 2015.

[7] J. M. Segura and I. Carol. Coupled hm analysis using zero-thickness interface elements with double nodes. Part I: Theoretical model. *International Journal for Numerical and Analytical Methods in Geomechanics*, 32(18):2083–2101, 2008.

[8] T. J. Boone and A. R. Ingraffea. A numerical procedure for simulation of hydraulically-driven fracture propagation in poroelastic media. *Int. J. for Numer. Analyt. Meth. in Geomechanics*, 14(1):27–47, 1990.

[9] R. E. Goodman, R. L. Taylor, and T. L. Brekke. A model for the mechanics of jointed rock. *Journal of the Soil Mechanics and Foundation Division*, 94:637–659, 1968.

[10] O. Zienkiewicz and R. Taylor. *The finite element method.*, volume I. McGraw Hill, 2000.